

# Analysis of three conductor coaxial systems : computer-aided determination of the frequency characteristics and the impulse and step response of a two-port consisting of a system of three coaxial conductors terminating in lumped impedances

**Citation for published version (APA):**

van der Plaats, J. (1975). *Analysis of three conductor coaxial systems : computer-aided determination of the frequency characteristics and the impulse and step response of a two-port consisting of a system of three coaxial conductors terminating in lumped impedances*. (EUT report. E, Fac. of Electrical Engineering; Vol. 75-E-56). Technische Hogeschool Eindhoven.

**Document status and date:**

Published: 01/01/1975

**Document Version:**

Publisher's PDF, also known as Version of Record (includes final page, issue and volume numbers)

**Please check the document version of this publication:**

- A submitted manuscript is the version of the article upon submission and before peer-review. There can be important differences between the submitted version and the official published version of record. People interested in the research are advised to contact the author for the final version of the publication, or visit the DOI to the publisher's website.
- The final author version and the galley proof are versions of the publication after peer review.
- The final published version features the final layout of the paper including the volume, issue and page numbers.

[Link to publication](#)

**General rights**

Copyright and moral rights for the publications made accessible in the public portal are retained by the authors and/or other copyright owners and it is a condition of accessing publications that users recognise and abide by the legal requirements associated with these rights.

- Users may download and print one copy of any publication from the public portal for the purpose of private study or research.
- You may not further distribute the material or use it for any profit-making activity or commercial gain
- You may freely distribute the URL identifying the publication in the public portal.

If the publication is distributed under the terms of Article 25fa of the Dutch Copyright Act, indicated by the "Taverne" license above, please follow below link for the End User Agreement:

[www.tue.nl/taverne](http://www.tue.nl/taverne)

**Take down policy**

If you believe that this document breaches copyright please contact us at:

[openaccess@tue.nl](mailto:openaccess@tue.nl)

providing details and we will investigate your claim.

Download date: 04. Oct. 2023

th

e

Analysis of three conductor coaxial systems.

Computer-aided determination of the frequency characteristics and the impulse and step response of a two-port consisting of a system of three coaxial conductors terminating in lumped impedances.

Analysis of three conductor coaxial systems.

Computer-aided determination of the frequency characteristics and the impulse and step response of a two-port consisting of a system of three coaxial conductors terminating in lumped impedances.

by

J. van der Plaats

TECHNISCHE HOGESCHOOL EINDHOVEN

NEDERLAND

AFDELING DER ELEKTROTECHNIEK

VAKGROEP TELECOMMUNICATIE

EINDHOVEN UNIVERSITY OF TECHNOLOGY

THE NETHERLANDS

DEPARTMENT OF ELECTRICAL ENGINEERING

GROUP TELECOMMUNICATIONS

Analysis of three conductor  
coaxial systems.

Computer-aided determination of the  
frequency characteristics and the  
impulse and step response of a two-port  
consisting of a system of three coaxial  
conductors terminating in lumped impedances.

by

J. van der Plaats

TH-Report 75-E-56

March 1975

ISBN 90 6144 056 4

## Contents

1. Summary	1
2. Introduction	2
2.1 Object of the analysis	2
2.2 Description of the system	2
2.3 Nomenclature	4
3. Derivation of the field intensities from Maxwell's equations	5
3.1 General formulae describing the system	5
3.2 Field intensities in the conductors	6
3.3 Field intensities in the dielectrics	6
4. The field intensities in the three conductors and the two dielectrics expressed in terms of the currents $I_1$ and $I_2$	8
4.1 Field intensities in conductor 1	8
4.2 Field intensities in dielectric a	9
4.3 Field intensities in conductor 2	9
4.4 Field intensities in the dielectric b	10
4.5 Field intensities in conductor 3	11
5. The propagation modes	13
5.1 Derivation of the propagation constants belonging to the different possible propagation modes	13
5.2 Current ratios and voltage ratios corresponding to the four propagation modes	14
6. Currents and voltages in the system	16
6.1 General equations of currents and voltages	16
6.2 Introduction of a certain set of terminal conditions	16
7. Description of the overall behaviour of the system in the frequency and the time domains	18
7.1 Eigenvalue of the system, transfer impedance $H(\omega)$	18
7.2 Impulse response and step response of the system	18
8. Computational results	20
8.1 A coaxial shunt 1 metre in length	20
8.2 A coaxial shunt 3 metre in length	21
9. Conclusions	32
10. Acknowledgement	33
11. References	34

## 1. Summary

A theoretical analysis is presented of a system consisting of three coaxial conductors of a certain length terminating in concentrated elements. This is a configuration which is applied in coaxial shunts. Starting with Maxwell's equations, expressions are derived, describing the field intensities in the conductors and in the intermediate dielectrics. The four quasi TEM propagation modes, inherent in three parallel conductors, are derived from the characteristic determinant of the system and are used to obtain general expressions for the currents and the voltages in the system. After the introduction of the terminal conditions in conformity with the use of the system as a coaxial shunt, the eigenvalue  $H(\omega)$  of the two-port concerned is determined. The inverse Fourier transform then leads to the impulse response of the two-port from which the step response is derived by integration. Finally, computational results are given of the transfer impedance and the responses in the time domain.

## 2. Introduction

### 2.1 Object of the analysis

The object of the investigations described in this paper is to derive the responses in the frequency domain as well as in the time domain of a structure consisting of two coaxial pairs coupled to each other by a common cylindrical conductor.

The direct motive for these investigation was the possibility of analysing the behaviour of the coaxial shunt making use of the experience gained in the author's research group in treating coaxial structures.

A coaxial shunt is a device with the structure mentioned and is used for measuring high short-circuit currents [3].

Because a reliable interpretation of a measured transient response of a coaxial shunt requires a precise knowledge of the behaviour of the system, a general fundamental analysis of the structure seemed justifiable.

Moreover, the same basic configuration is used to measure the transfer impedance of coaxial cables, an important quantity related to crosstalk in coaxial cable systems [4].

The treatment is distinguished from others [3],[6],[7] in several ways :

- a. It takes as a starting point the very coaxial structure and not a substitute with concentrated elements.
- b. There is no restriction as regards the thickness of the common conductor.
- c. There are no restrictions as to frequency intervals.
- d. Complete transient responses are calculated with discrete Fourier transforms [5].

### 2.2 Description of the system

The investigated system consists of three parallel conductors of the same length, at both ends arbitrarily terminating in concentrated elements. The system is excited by one or more voltage and/or current sources at one or both ends of the system.

Fig. 1 shows a possible situation with a single voltage source.

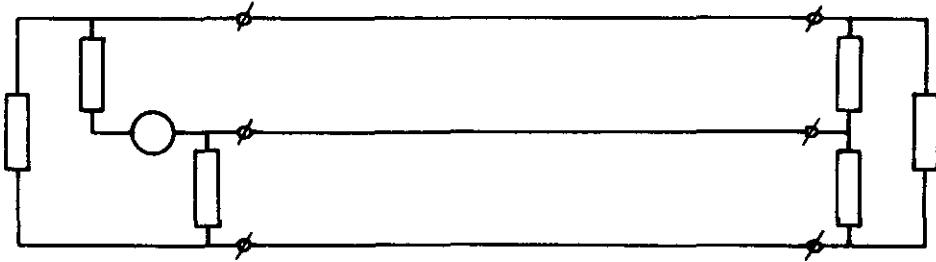


Fig. 1. Principle of the system, consisting of three parallel conductors, terminating in concentrated elements and driven by one or more voltage and/or current sources

With regard to the conductors, it is assumed that there are three mutually isolated, coaxial, cylindrical conductors, one massive one surrounded by two hollow conductors, as shown in fig. 2.

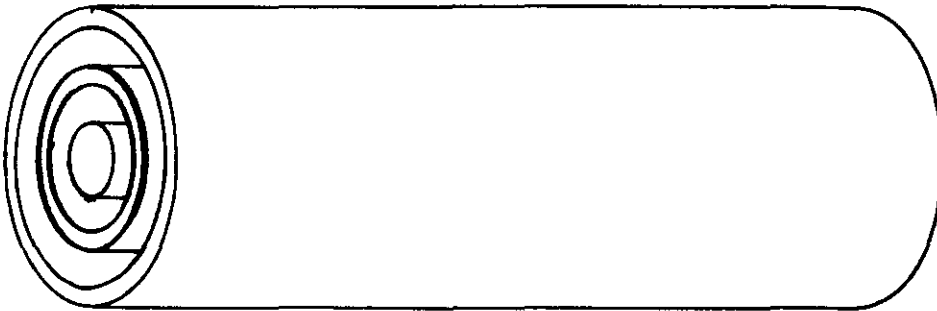


Fig. 2. The physical construction of the three parallel conductors

With regard to the terminations and the kind of excitation, we will restrict ourselves to the situation as sketched in fig. 3.

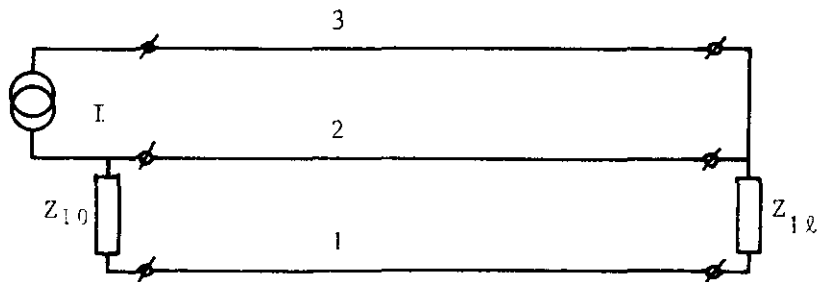


Fig. 3. The assumed terminal conditions

The outer coaxial pair, consisting of the conductors 2 and 3, is short-circuited at one end and excited by a current source at the other.

The main part of the injected current  $I$  takes its way through the common conductor 2 and the rest takes its way through the inner conductor 1; the total current  $I$  flows back through the outer conductor 3.

The inner coaxial pair (conductors 1 and 2) in general terminates in impedances  $Z_{10}$  and  $Z_{1g}$ . In practice,  $Z_{10}$  will be zero (a short circuited end) or will be taken equal to the high frequency characteristic impedance of the inner coaxial pair.

$Z_{1g}$ , the impedance across which the output voltage is measured if the system is used as a coaxial shunt, can be an open end or, for instance, a resistor, equalling the high-frequency characteristic impedance of the inner pair. Other kinds of terminations than the ones treated do not give rise to new aspects and can be solved in the same way.

### 2.3 Nomenclature

The most elegant way to describe the rotational symmetrical system concerned is by means of cylindrical polar co-ordinates  $(\rho, \phi, z)$ .

Let the  $z$ -axis coincide with the axis of the system. Distances to the axis are then represented by  $\rho$ . As a result of the rotational symmetry all the physical magnitudes are independent of  $\phi$ .

From the axis to the outside of the system the conductors will be indicated by 1, 2 and 3 and the dielectrics by  $a$  and  $b$  (fig. 4).

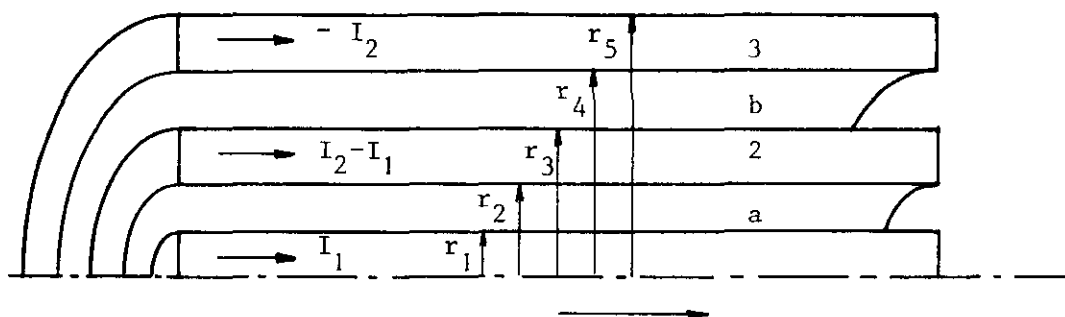


Fig. 4. The nomenclature of the system of three coaxial conductors

The respective radii will be denoted by  $r_1$  to  $r_5$ .

The currents in the positive  $z$ -direction are denoted by  $I_1$  in conductor 1,  $I_2 - I_1$  in conductor 2, and  $-I_2$  in conductor 3 respectively. The sum of these currents being zero, there will be no resulting field outside the system.



### 3. Derivation of the field intensities from Maxwell's equations

#### 3.1 General formulae describing the system.

The starting point is found in Maxwell's equations :

$$\nabla \times H = gE + \frac{\delta D}{\delta t} \quad (1)$$

$$\nabla \times E = - \frac{\delta B}{\delta t} \quad (2)$$

$$B = \mu H \quad (3)$$

$$D = \epsilon E \quad (4)$$

If all the time-dependent magnitudes are supposed to be sinusoidal functions of time and independent of  $\phi$ , a change to cylindrical co-ordinates leads to :

$$\frac{\delta H_{\phi}}{\delta z} = -(g + j\omega\epsilon)E_{\rho} \quad (5)$$

$$\frac{\delta(\rho H_{\phi})}{\delta \rho} = (g + j\omega\epsilon)\rho E_z \quad (6)$$

$$\frac{\delta E_z}{\delta \rho} - \frac{\delta E_{\rho}}{\delta z} = j\omega\mu H_{\phi} \quad (7)$$

The formulae (5) (6) and (7) are valid in the conductors as well as in the dielectrics.

Substitution of (5) and (6) in (7) results in :

$$\frac{\delta}{\delta \rho} \left[ \frac{1}{\rho} \frac{\delta(\rho H_{\phi})}{\delta \rho} \right] + \frac{\delta^2 H_{\phi}}{\delta z^2} = (j\omega\mu g - \omega^2 \epsilon \mu) H_{\phi} \quad (8)$$

Using the normal method of searching for particular solutions,  $H_{\phi}$  is written as a product of two functions, the first a function of  $z$  alone and the other a function of  $\rho$  alone. The dependence on  $z$  is then found to be given by :

$$H_{\phi}(\rho, z) = H_{\phi}(\rho) \cdot e^{-\gamma z} \quad (9)$$

supposing (for the sake of simplicity) only for the time being a wave in the positive  $z$ -direction.

### 3.2 Field intensities in the conductors

As the displacement current in metals is very small compared with the conduction current, it is allowed to put  $\epsilon=0$ ; this is certainly allowed for all the frequencies that play a role in the calculations to be made in this paper.

Substituting  $\epsilon=0$  and the time-dependence given by (9) in (8) gives :

$$\frac{d}{d\rho} \left[ \frac{1}{\rho} \frac{d(\rho H_{\phi})}{d\rho} \right] = (\sigma^2 - \gamma^2) H_{\phi} \quad (10)$$

with  $\sigma^2 = j\omega\mu g$  (11)

In all practical situations, if the conductors are made of metals (for instance copper with  $g=5,8 \cdot 10^7 \Omega^{-1} m^{-1}$ )

$\gamma^2$  can be ignored compared with  $\sigma^2$ , so (10) can be written as :

$$\frac{d^2 H_{\phi}}{d\rho^2} + \frac{1}{\rho} \frac{dH_{\phi}}{d\rho} - \frac{1}{\rho^2} H_{\phi} = \sigma^2 H_{\phi} \quad (12)$$

The solution of (12) yields

$$H_{\phi} = A I_1(\sigma\rho) + B K_1(\sigma\rho) \quad (13)$$

which is a summation of two Bessel functions.

From (6) and (5) respectively follows :

$$E_z = \frac{\sigma}{g} [A I_0(\sigma\rho) - B K_0(\sigma\rho)] \quad (14)$$

$$E_{\rho} = \frac{\gamma}{g} H_{\phi} \approx 0$$

### 3.3 Field intensities in the dielectrics

If the isolating media between the conductors are of such a quality that the conductivity can be ignored (for instance air, polyethylene), the equations (5), (6) and (7), after introducing the z-dependence given by (9), become

$$E_z = \frac{\gamma}{j\omega\epsilon} H_{\phi} \quad (16)$$

$$\frac{d(\rho H_{\phi})}{d\rho} = j\omega\epsilon\rho E_z \quad (17)$$

$$\frac{dE_z}{d\rho} + \gamma E_z = j\omega\mu H_{\phi} \quad (18)$$

The conduction current resulting from  $E_z$  being very small compared with the current in the conductors, it can be put that the magnetomotive intensity  $H_\phi$  in the dielectrics is only determined by the currents in the conductors, leading to :

$$H_\phi = \frac{I_t}{2\pi\rho} \quad (19)$$

with  $I_t$  the total enclosed current in the conductors by the field line concerned. It is thus supposed that :

$$\frac{d(\rho H_\phi)}{d\rho} = 0 \quad (20)$$

an approximation of (17).

Substitution of (16) in (18) and solution of the resulting differential equation gives :

$$E_z = \frac{1}{2\tau} \left( j\omega\mu - \frac{\gamma^2}{j\omega\epsilon} \right) I_t \ln \frac{\rho}{r_n} + E_z(r_n) \quad (21)$$

for  $r_n \leq \rho \leq r_{n+1}$

with  $r_n$  the radius of the nearest enclosed metal-insulator interface. The expression derived can now be used in the particular case of the three mutually isolated coaxial conductors, as described below.

4. The field intensities in the three conductors and the two dielectrics expressed in terms of the currents  $I_1$  and  $I_2$ .

The general expressions derived in part 3 can now be used to find specific solutions to the particular case of the coaxial conductors. This means that the constants in the formulae have to be expressed in terms of the currents  $I_1$  and  $I_2$ . It is assumed that the conductors 1, 2 and 3 have the constants  $\sigma_1$ ,  $\sigma_2$  and  $\sigma_3$  because it is not necessary for the conductivity of the conductors to be equal.

Used as a coaxial shunt, for instance, it is imaginable that the common conductor 2 is made of a material with a high specific resistance and the conductors 1 and 3 of a material with a low specific resistance.

As in the general case the constants in formulae (13) and (14) were denoted by A and B, in the specific cases they will be represented by  $A_1$  and  $B_1$  in conductor 1,  $A_2$  and  $B_2$  in conductor 2, etc.

4.1 Field intensities in conductor 1

With the restriction that the formulae hold only for  $0 \leq \rho \leq r_1$ , (13) becomes

$$H_\phi = A_1 I_1(\sigma_1 \rho) + B_1 K_1(\sigma_1 \rho) \quad (22)$$

$$\sigma_1^2 = j\omega\mu g_1 \quad (23)$$

Because  $K_1(\sigma_1 \rho)$  is infinite for  $\rho=0$ , it follows that  $B_1=0$ . With  $\rho=r_1$  in (19) it follows from (22) that :

$$A_1 = \frac{I_1}{2\pi r_1} \cdot \frac{1}{I_1(\sigma_1 r_1)} \quad (24)$$

With (24) and  $B_1=0$  substituted in (22) and (14), the latter read

$$H_\phi = I_1 \frac{I_1(\sigma_1 \rho)}{2\pi r_1 I_1(\sigma_1 r_1)} \quad (25)$$

$$E_z = r_1 I_1 \frac{I_0(\sigma_1 \rho)}{2\pi r_1 I_1(\sigma_1 r_1)} \quad (26)$$

$$\text{with } r_{11} = \frac{\sigma_1}{g_1} \quad (27)$$

On the interface between 1 and a we have :

$$E_z(r_1) = \eta_1 I_1 \frac{I_0(\sigma_1 r_1)}{2\pi r_1 I_1(\sigma_1 r_1)} = W I_1 \quad (28)$$

with 
$$W = \frac{I_0(\sigma_1 r_1)}{2\pi r_1 I_1(\sigma_1 r_1)} \cdot \eta_1 \quad (29)$$

#### 4.2 Field intensities in dielectric a

In the interval  $r_1 \leq \rho \leq r_2$  (19) becomes :

$$H_\phi = \frac{I_1}{2\pi\rho} \quad (30)$$

From (16) and (30) it follows that :

$$E_\rho = \frac{\gamma I_1}{2\pi j\omega\epsilon\rho} \quad (31)$$

And from (21)

$$E_z = \frac{1}{2\pi} (j\omega L - \frac{\gamma^2}{j\omega\epsilon}) I_1 \ln \frac{\rho}{r_1} + E_z(r_1) \quad (32)$$

With (28) substituted in (32) :

$$E_z = \left\{ \frac{1}{2\pi} (j\omega\mu - \frac{\gamma^2}{j\omega\epsilon}) \ln \frac{\rho}{r_1} + W \right\} I_1 \quad (33)$$

#### 4.3 Field intensities in conductor 2

The magnetic field intensity in conductor 2 follows from (13) by substituting  $A_2$ ,  $B_2$  and  $\sigma_2$  for  $A$ ,  $B$  and  $\sigma$ :

$$H_\phi = A_2 I_1(\sigma_2 \rho) + B_2 K_1(\sigma_2 \rho) \quad (34)$$

for  $r_2 \leq \rho \leq r_3$

In the special cases in which  $\rho=r_2$  and  $\rho=r_3$  (34) becomes with (19)

$$A_2 I_1(\sigma_2 r_2) + B_2 K_1(\sigma_2 r_2) = \frac{I_1}{2\pi r_2} \quad \text{and} \quad (35)$$

$$A_2 I_1(\sigma_2 r_3) + B_2 K_1(\sigma_2 r_3) = \frac{I_2}{2\pi r_3} \quad (36)$$

respectively.

Solving  $A_2$  and  $B_2$  from (35) and (36) we obtain :

$$A_2 = \frac{I_1}{2\pi r_2} \cdot \frac{K_1(\sigma_2 r_3)}{D_2} - \frac{I_2}{2\pi r_3} \cdot \frac{K_1(\sigma_2 r_2)}{D_2} \quad (37)$$

$$B_2 = -\frac{I_1}{2\pi r_2} \cdot \frac{I_1(\sigma_2 r_3)}{D_2} + \frac{I_2}{2\pi r_3} \cdot \frac{I_1(\sigma_2 r_2)}{D_2} \quad (38)$$

$$\text{With } D_2 = I_1(\sigma_2 r_2)K_1(\sigma_2 r_3) - I_1(\sigma_2 r_3)K_1(\sigma_2 r_2) \quad (39)$$

From (14) it follows that :

$$E_z = \eta_2 \{A_2 I_0(\sigma_2 \rho) - B_2 K_0(\sigma_2 \rho)\} \quad (40)$$

On the interface between a and 2 :

$$E_z(r_2) = F I_1 - G I_2 \quad (41)$$

With :

$$F = \frac{I_0(\sigma_2 r_2)K_1(\sigma_2 r_3) + I_1(\sigma_2 r_3)K_0(\sigma_2 r_2)}{2\pi r_2 D_2} \cdot \eta_2 \quad (42)$$

$$G = \frac{I_0(\sigma_2 r_2)K_1(\sigma_2 r_2) + I_1(\sigma_2 r_2)K_0(\sigma_2 r_2)}{2\pi r_3 D_2} \cdot \eta_2 \quad (43)$$

The axial component of the electric field intensity on the interface between a and 2 can also be found from (33) :

$$E_z(r_2) = \left\{ \frac{1}{2\pi} (j\omega\mu - \frac{\gamma^2}{j\omega\epsilon}) \ln \frac{r_2}{r_1} + W \right\} I_1 \quad (44)$$

Elimination of  $E_z(r_2)$  from (41) and (44) gives an equation in terms of  $I_1$  and  $I_2$  with parameter  $\gamma$  :

$$\left\{ \frac{1}{2\pi} (j\omega\mu - \frac{\gamma^2}{j\omega\epsilon}) \ln \frac{r_2}{r_1} - F + W \right\} I_1 + G I_2 = 0 \quad (45)$$

#### 4.4 Field intensities in the dielectric b

For the dielectric b, if  $r_3 \leq \rho \leq r_4$ , it follows from (19) that :

$$H_\phi = \frac{I_2}{2\pi\rho} \quad (46)$$

And from (16) together with (46) :

$$E_\rho = \frac{\gamma I_2}{2\rho j\omega\epsilon\rho} \quad (47)$$

From (21) it follows that :

$$E_z = \frac{1}{2\pi} (j\omega\mu - \frac{\gamma^2}{j\omega\epsilon}) I_2 \ln \frac{\rho}{r_3} + E_z(r_3) \quad (48)$$

The component of the electric field-intensity  $E_z(r_3)$  follows from (40) :

$$E_z(r_3) = r_2 \{A_2 I_0(\sigma_2 r_3) - B_2 K_0(\sigma_2 r_3)\} \quad (49)$$

(49) in (48) gives :

$$E_z = \frac{1}{2\pi} (j\omega\mu - \frac{\gamma^2}{j\omega\epsilon}) I_2 \ln \frac{\rho}{r_3} + r_2 \{A_2 I_0(\sigma_2 r_3) - B_2 K_0(\sigma_2 r_3)\} \quad (50)$$

#### 4.5 Field intensities in conductor 3

The magnetic field intensity in conductor 3 follows from (13) by substituting  $A_3$ ,  $B_3$  and  $\sigma_3$  for A, B and  $\sigma$ :

$$H_\phi = A_3 I_1(\sigma_3 \rho) + B_3 K_1(\sigma_3 \rho) \quad (51)$$

for  $r_4 \leq \rho \leq r_5$

In the special cases in which  $\rho=r_4$  and  $\rho=r_5$  (51) becomes with (19) :

$$A_3 I_1(\sigma_3 r_4) + B_3 K_1(\sigma_3 r_4) = \frac{I_2}{2\pi r_4} \quad \text{and} \quad (52)$$

$$A_3 I_1(\sigma_3 r_5) + B_3 K_1(\sigma_3 r_5) = 0 \quad (53)$$

respectively.

Solving  $A_3$  and  $B_3$  from (52) and (53) we obtain :

$$A_3 = \frac{I_2}{2\pi r_4} \cdot \frac{K_1(\sigma_3 r_5)}{D_3} \quad (54)$$

$$B_3 = - \frac{I_2}{2\pi r_4} \cdot \frac{I_1(\sigma_3 r_5)}{D_3} \quad (55)$$

With :

$$D_3 = I_1(\sigma_3 r_4) K_1(\sigma_3 r_5) - I_1(\sigma_3 r_5) K_1(\sigma_3 r_4) \quad (56)$$

From (14) it follows that :

$$E_z = r_3 \{A_3 I_0(\sigma_3 \rho) - B_3 K_0(\sigma_3 \rho)\} \quad (57)$$

On the interface between b and 3 :

$$E_z(r_4) = LI_2 \quad (58)$$

With :

$$L = \frac{I_0(\sigma_3 r_4) K_1(\sigma_3 r_5) + I_1(\sigma_3 r_5) K_0(\sigma_3 r_4)}{2\pi r_4 D_3} \cdot n_3 \quad (59)$$

$E_z(r_4)$  can also be found from (50) :

$$E_z(r_4) = \frac{1}{2\pi} (j\omega\mu - \frac{\gamma^2}{j\omega\epsilon}) I_2 \ln \frac{r_4}{r_3} + MI_1 - NI_2 \quad (60)$$

with

$$M = \frac{I_0(\sigma_2 r_3) K_1(\sigma_2 r_3) + I_1(\sigma_2 r_3) K_0(\sigma_2 r_3)}{2\pi r_2 D_2} \cdot n_2 \quad (61)$$

$$N = \frac{I_0(\sigma_2 r_3) K_1(\sigma_2 r_2) + I_1(\sigma_2 r_2) K_0(\sigma_2 r_3)}{2\pi r_3 D_2} \cdot n_2 \quad (62)$$

Elimination of  $E_z(r_4)$  from (59) and (60) gives a second equation in terms of  $I_1$  and  $I_2$  with  $\gamma$  as parameter.

$$MI_1 + \left\{ \frac{1}{2\pi} (j\omega\mu - \frac{\gamma^2}{j\omega\epsilon}) \ln \frac{r_4}{r_3} - L - N \right\} I_2 = 0 \quad (63)$$



5. The propagation modes

5.1 Derivation of the propagation constants belonging to the different possible propagation modes

The equations (45) and (63) form a set of two homogeneous linear equations in the unknowns  $I_1$  and  $I_2$ . A necessary and sufficient condition for this set of equations to have a solution other than the trivial one  $I_1=I_2=0$ , is that the characteristic determinant of the coefficients must vanish, that is :

$$\begin{vmatrix} \frac{1}{2\pi}(j\omega\mu - \frac{\gamma^2}{j\omega\epsilon}) \ln \frac{r_2}{r_1} - F + W & G \\ M & \frac{1}{2\pi}(j\omega\mu - \frac{\gamma^2}{j\omega\epsilon}) \ln \frac{r_4}{r_3} - L - N \end{vmatrix} = 0 \quad (64)$$

With  $Q = \frac{j\pi}{\omega\mu \ln \frac{r_2}{r_1} \ln \frac{r_4}{r_3}}$  (65)

$$O_1 = (L+N) \ln \frac{r_2}{r_1} \quad (66)$$

$$O_2 = (F-W) \ln \frac{r_4}{r_3} \quad (67)$$

$$O = (O_1 - O_2)^2 + 4GM \ln \frac{r_2}{r_1} \ln \frac{r_4}{r_3} \quad (68)$$

$$P = O_1 + O_2 \quad (69)$$

$$B_i = \omega\mu\epsilon \quad (70)$$

the solutions of (64) become :

$$\gamma_1 = \pm jB_i \{1 + Q(P - O^{\frac{1}{2}})\}^{\frac{1}{2}} \quad (71)$$

$$\gamma_2 = \pm jB_i \{1 + Q(P + O^{\frac{1}{2}})\}^{\frac{1}{2}} \quad (72)$$

Each solution of  $\gamma$  corresponds to a propagation mode [1]. The currents and the voltages in the system are linear superpositions of the component waves of all the four modes of propagation, two of which propagate in the +z direction and two in the -z direction.

## 5.2 Current ratios and voltage ratios corresponding to the four propagation modes

To each mode corresponds a certain ratio between the currents  $I_1$  and  $I_2$ . Substitution of  $\gamma_1^2$  in (45) or in (63) gives us an expression for the corresponding current ratio  $k_1$  :

$$k_1 = \frac{I_2}{I_1} = \frac{jf\mu\{Q(P-O^{\frac{1}{2}})\}\ln \frac{r_2}{r_1} - F + W}{-G} \quad (76)$$

$$k_1 = \frac{I_2}{I_1} = \frac{-M}{jf\mu\{Q(P-O^{\frac{1}{2}})\}\ln \frac{r_4}{r_3} - L - N} \quad (77)$$

Substitution of  $\gamma_2^2$  in (45) or in (63) gives us an expression for the corresponding current ratio  $k_2$  :

$$k_2 = \frac{I_1}{I_2} = \frac{-G}{jf\mu\{Q(P+O^{\frac{1}{2}})\}\ln \frac{r_2}{r_1} - F + W} \quad (78)$$

$$k_2 = \frac{I_1}{I_2} = \frac{jf\mu\{Q(P+O^{\frac{1}{2}})\}\ln \frac{r_4}{r_3} - L - N}{-M} \quad (79)$$

(The current ratios have been so chosen that  $|k_1| < 1$  and  $|k_2| < 1$ )

The voltage  $V_a$  between conductor 1 and conductor 2 follows from an integration of  $E_\rho$  to  $c$  :

$$V_a = \int_{r_1}^{r_2} E_\rho d\rho \quad (80)$$

With (31) this becomes :

$$V_a = \int_{r_1}^{r_2} \frac{\gamma I_1}{2\pi j \omega \epsilon_\rho} d\rho = \frac{\gamma I_1}{2\pi j \omega \epsilon} \ln \frac{r_2}{r_1} \quad (81)$$

The voltage  $V_b$  between conductor 2 and conductor 3 follows with (47) :

$$V_b = \frac{\gamma I_2}{2\pi j \omega \epsilon} \cdot \ln \frac{r_4}{r_3} \quad (82)$$

The voltage ratio corresponding with  $\gamma_1$  :

$$\frac{V_b}{V_a} = \frac{I_2}{I_1} \cdot \frac{\ln \frac{r_4}{r_3}}{\ln \frac{r_2}{r_1}} = k_1 \frac{\ln \frac{r_4}{r_3}}{\ln \frac{r_2}{r_1}} \quad (83)$$

The voltage ratio corresponding with  $\gamma_2$  :

$$\frac{V_a}{V_b} = \frac{I_1}{I_2} \cdot \frac{\ln \frac{r_2}{r_1}}{\ln \frac{r_4}{r_3}} = k_2 \frac{\ln \frac{r_2}{r_1}}{\ln \frac{r_4}{r_3}} \quad (84)$$

## 6. The currents and voltages in the system

### 6.1 General equations of currents and voltages

In general, there will be a linear combination of the different voltages, respectively currents, corresponding to the four propagation modes.

This gives us the following general expressions for the voltages and the currents :

$$V_a = Z_{a_1} A \epsilon^{-\gamma_1 z} + B Z_{a_1} \epsilon^{\gamma_1 z} + k_2 Z_{a_2} C \epsilon^{-\gamma_2 z} + k_2 Z_{a_2} D \epsilon^{\gamma_2 z} \quad (80)$$

$$V_b = k_1 Z_{b_1} A \epsilon^{-\gamma_1 z} + k_1 Z_{b_1} B \epsilon^{\gamma_1 z} + Z_{b_2} C \epsilon^{-\gamma_2 z} + Z_{b_2} D \epsilon^{\gamma_2 z} \quad (81)$$

$$I_1 = A \epsilon^{-\gamma_1 z} - B \epsilon^{\gamma_1 z} + k_2 C \epsilon^{-\gamma_2 z} - k_2 D \epsilon^{\gamma_2 z} \quad (82)$$

$$I_2 = k_1 A \epsilon^{-\gamma_1 z} - k_1 B \epsilon^{\gamma_1 z} + C \epsilon^{-\gamma_2 z} - D \epsilon^{\gamma_2 z} \quad (83)$$

where

$$Z_{a_1} = \frac{\gamma_1}{2\pi j \omega \epsilon} \ln \frac{r_2}{r_1} \quad (84)$$

$$Z_{b_1} = \frac{\gamma_1}{2\pi j \omega \epsilon} \ln \frac{r_4}{r_3} \quad (85)$$

$$Z_{a_2} = \frac{\gamma_2}{2\pi j \omega \epsilon} \ln \frac{r_2}{r_1} \quad (86)$$

$$Z_{b_2} = \frac{\gamma_2}{2\pi j \omega \epsilon} \ln \frac{r_4}{r_3} \quad (87)$$

$Z_{a_1}$  and  $Z_{b_1}$  are the characteristic impedances ( $V_a/I_1$  and  $V_b/I_2$ ) of the inner and outer coaxial pairs, respectively if the propagation mode with propagation constant  $\gamma_1$  is the only mode present in the system.

$Z_{a_2}$  and  $Z_{b_2}$  are these characteristic impedances with  $\gamma_2$  as propagation constant.

### 6.2 Introduction of a certain set of terminal conditions

A solution of equations (80) to (83) to find the voltages  $V_a$  and  $V_b$  and of the currents  $I_1$  and  $I_2$ , is only possible if the constants A, B, C and D are known.

Because the values of these constants follow from the terminal conditions, we now choose the concrete situation that is shown in fig. 5. These conditions correspond with the use of the system as a coaxial shunt for current measuring purposes and were also the starting point for the calculations that led to the results described in section 8 of this paper.

From fig. 5 we see that the terminal conditions read :

$$\text{For } z=0 \quad I_2 = I \quad (88)$$

$$V_a = 0 \quad (89)$$

$$\text{For } z=l \quad V_b = 0 \quad (90)$$

$$I_1 R = V_a \quad (91)$$

(88) substituted in (83) gives us :

$$k_1 A - k_1 B + C - D = I \quad (92)$$

(89) substituted in (80) :

$$Z_{a_1} A + Z_{a_1} B + k_2 Z_{a_2} C + k_2 Z_{a_2} D = 0 \quad (93)$$

(90) substituted in (81)

$$k_1 Z_{b_1} A e^{-\gamma_1 l} + k_1 Z_{b_1} B e^{\gamma_1 l} + Z_{b_2} C e^{-\gamma_2 l} + Z_{b_2} D e^{\gamma_2 l} = 0 \quad (94)$$

(91) in (80) :

$$R(A e^{-\gamma_1 l} - B e^{\gamma_1 l} + k_2 C e^{-\gamma_2 l}) = Z_{a_1} A e^{-\gamma_1 l} + B Z_{a_1} e^{\gamma_1 l} + k_2 Z_{a_2} C e^{-\gamma_2 l} + k_2 Z_{a_2} D e^{\gamma_2 l} \quad (95)$$

The constants A, B, C and D can now be determined from (92) to (95) and substituted in the equations (80) to (83), giving explicit expressions for the voltages and currents as functions of z.

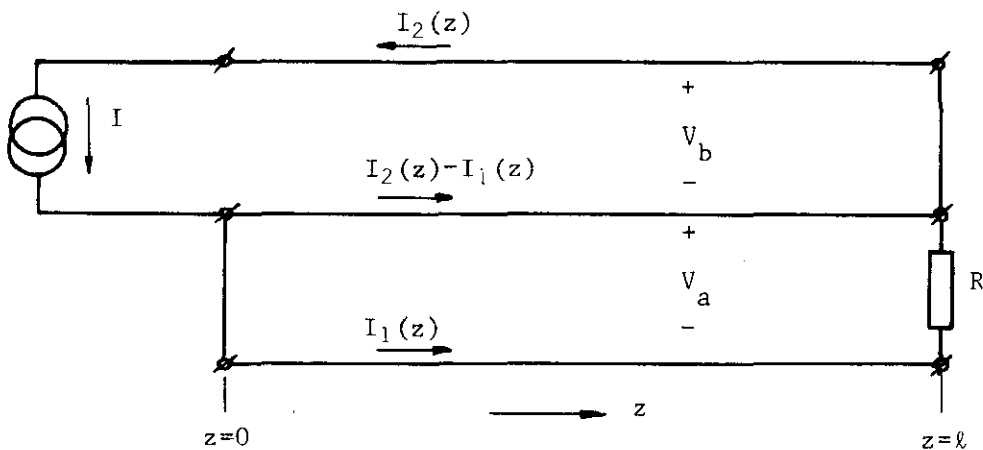


Fig. 5. The terminal conditions chosen

7. Description of the overall behaviour of the system in the frequency and in the time domains

7.1 Eigenvalue of the system, the transfer impedance  $H(\omega)$

Referring to fig.5, an impressed current  $I$  at  $z=0$  in the outer coaxial pair causes a voltage  $V_a(\ell)$  at  $z=\ell$  across the resistor  $R$  that terminates the inner coaxial pair. The system can thus be seen as a two-port (fig. 6) that can be described in the frequency domain by an eigenvalue, the transfer impedance  $H(\omega)$  defined as :

$$H(\omega) = \frac{V_a(\ell)}{I} \quad (96)$$

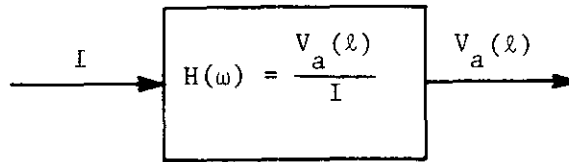


Fig. 6. The coaxial shunt as a two-port with driving current  $I$  and resulting voltage  $V_a(\ell)$ . The transfer impedance is defined as the quotient  $V_a(\ell)$  over  $I$ .

7.2 Impulse response and step response of the system

The impulse response  $h(t)$  of the system follows from the inverse Fourier transform of the transfer impedance :

$$h(t) = \frac{1}{2\pi} \int_{-\infty}^{\infty} H(\omega) e^{j\omega t} d\omega \quad (97)$$

It is the response of the system to the generalised function  $\delta(t)$ , the Dirac impulse.

The step response of the system follows by integrating the impulse response :

$$a(t) = \int_0^{\infty} h(t) dt \quad (98)$$

Because it is impossible to write  $H(\omega)$  in a closed mathematical form, the values of the transfer impedance are calculated for the discrete frequencies :  $r \cdot \Delta f$ , where  $r = 0, 1, 2, \dots, N-1$ , and  $\Delta f$  the spacing between sample points in the frequency domain.

$f_g = (N-1)\Delta f$  is the highest frequency that is taken into account. This is schematically illustrated in fig. 7.

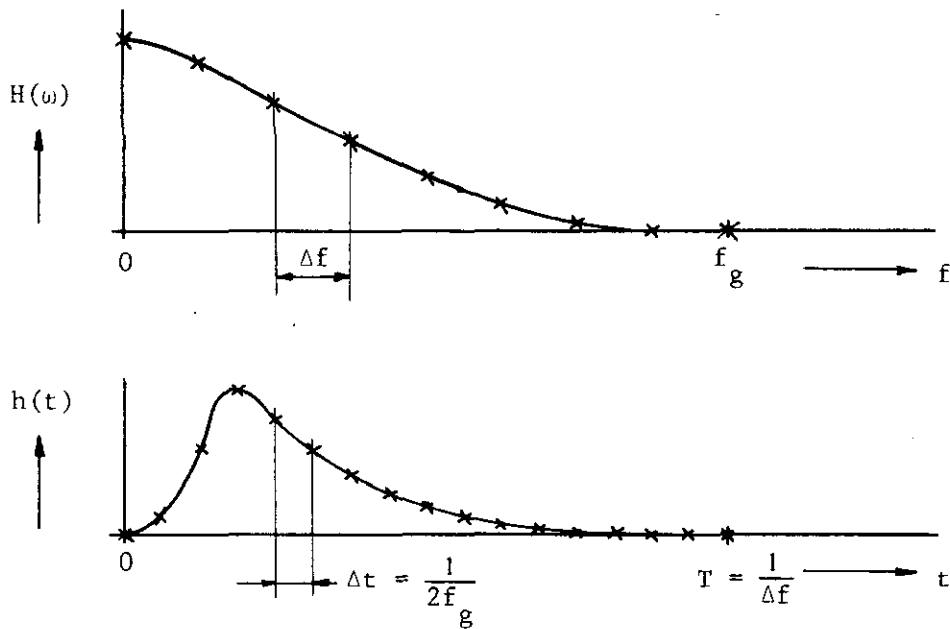


Fig. 7. The relations between  $\Delta t$  and  $f_g$  and between  $T$  and  $\Delta f$

The inverse discrete Fourier transform results in sample values of the impulse response, with a distance between the samples of

$$\Delta t = \frac{1}{2f_g}$$

The desired fine-structure of the impulse response can be achieved by taking the value of  $f_g$  sufficiently high.

Because the transform results in a periodic time-function, with a period

$$T = \frac{1}{\Delta f}$$

it is necessary to take care that the neighbouring pulses do not interfere. To avoid this "aliasing distortion" it is necessary to take  $\Delta f$  sufficiently low.

The Fourier transform mentioned is executed as a "Fast Fourier Transform", an efficient algorithm of the discrete Fourier transform [5].

## 8. Computational results

### 8.1 A coaxial shunt 1 metre in length

In this section graphical results are given of computations on a coaxial shunt with the following dimensions and constants :

$$\begin{array}{ll} \ell = 1 \text{ m} & r_1 = 4.13 \cdot 10^{-3} \text{ m} \\ g = 1,16 \cdot 10^6 \text{ S/m} & r_2 = 9.5 \cdot 10^{-3} \text{ m} \\ R = 50 \ \Omega & r_3 = 10.0 \cdot 10^{-3} \text{ m} \\ & r_4 = 23.0 \cdot 10^{-3} \text{ m} \\ & r_5 = 23.5 \cdot 10^{-3} \text{ m} \end{array}$$

The ratios  $r_2/r_1$  and  $r_4/r_3$  are so chosen that the high frequency characteristic impedances of the inner and outer pairs equal  $50 \ \Omega$ , with the idea that, at least for the higher frequencies, the system can be matched to a  $50 \ \Omega$  extension cable.

Fig. 8a gives an overall impression of the calculated amplitude characteristic that is a plot of  $\left| \frac{V_a(\ell)}{I} \right|$  as a function of frequency.

Fig. 8b gives the low frequency part of the amplitude characteristic.

An interesting part of this characteristic is found around the frequency of 75 MHz, corresponding with the coaxial shunt as a quarter-wavelength line.

Fig.9a and fig.9b show the real and imaginary parts of the transfer impedance respectively, and fig. 10 is the polar plot of the transfer impedance in the complex plane.

Fig. 11a gives an overall impression of the derived impulse response of the two-port, and fig. 11b the first part of this response.

The plot of fig. 11a makes clear that the sample density in the frequency domain is high enough to avoid aliasing distortion of the impulse response. To avoid unnecessary extra labour in the computation of the responses in the time domain, it is assumed that the transfer impedance equals zero for frequencies higher than 100 MHz, an assumption which is not entirely justifiable in the neighbourhood of frequencies corresponding with an odd number of quarter wavelengths.



The high frequency components which are thus ignored would slightly modify the appearance of the ripple on the impulse response.

Finally, fig. 12 shows the step response derived by integrating the impulse response.

## 8.2 A coaxial shunt 3 metres in length

To illustrate the influence of the length of the shunt on the responses, results are given of computations on a coaxial shunt with a length of 3 m. All the other dimensions and constants are kept the same as in the example of section 8.1.

Figures 13 to 17 give a clear insight into the behaviour of the coaxial shunt.

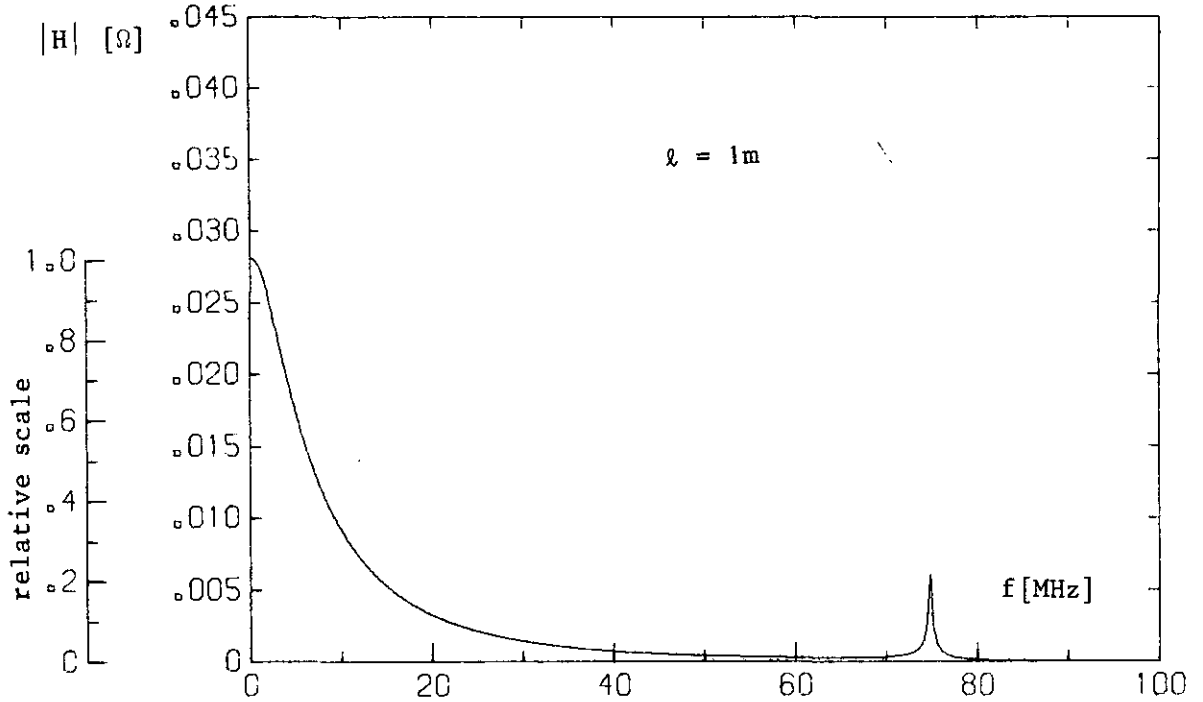


Fig.8a. The amplitude characteristic of the transfer impedance, that is  $|H|=|V_a(l)/I|$  as a function of frequency in 1000 steps of  $10^5$  Hz. Note the peak at 75 MHz, corresponding with the shunt as a quarter wavelength line.

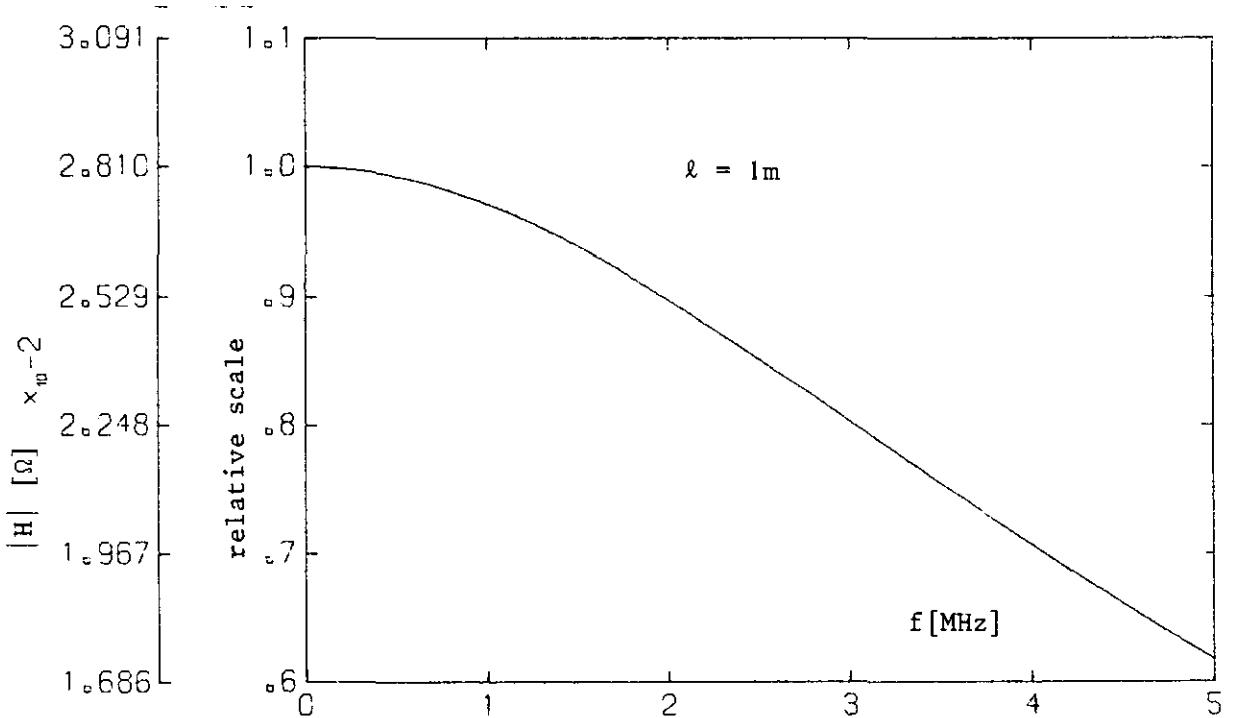


Fig.8b. The low frequency part of the amplitude characteristic calculated in 100 steps of  $5 \cdot 10^4$  Hz

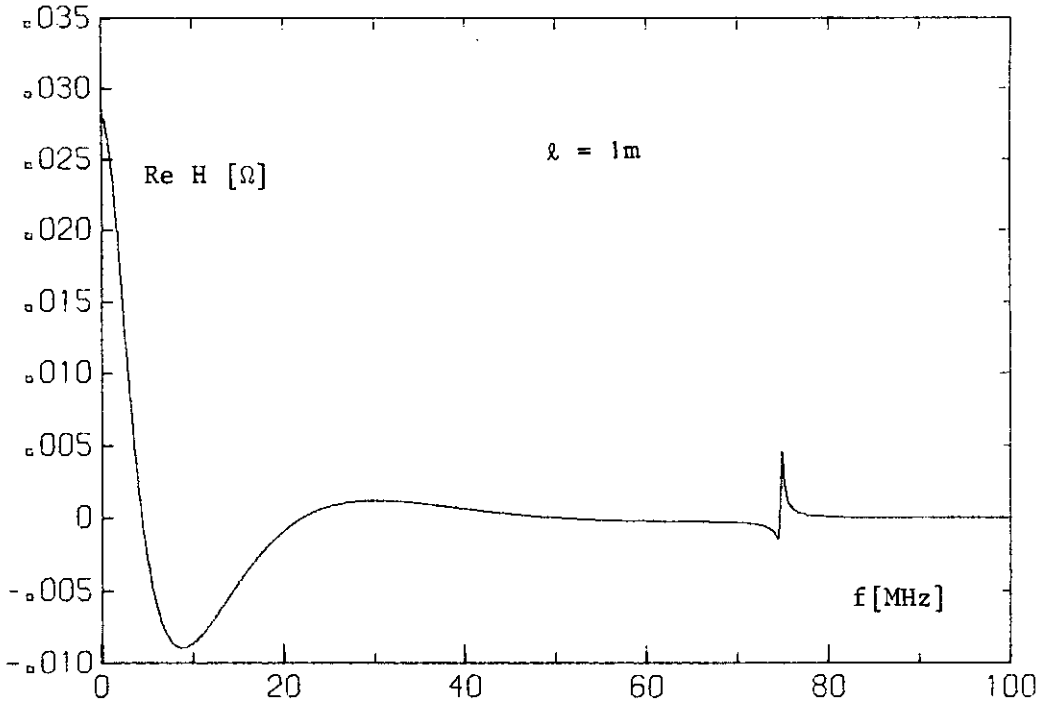


Fig.9a. The real part of the transfer impedance as a function of frequency in 1000 steps of  $10^5$  Hz

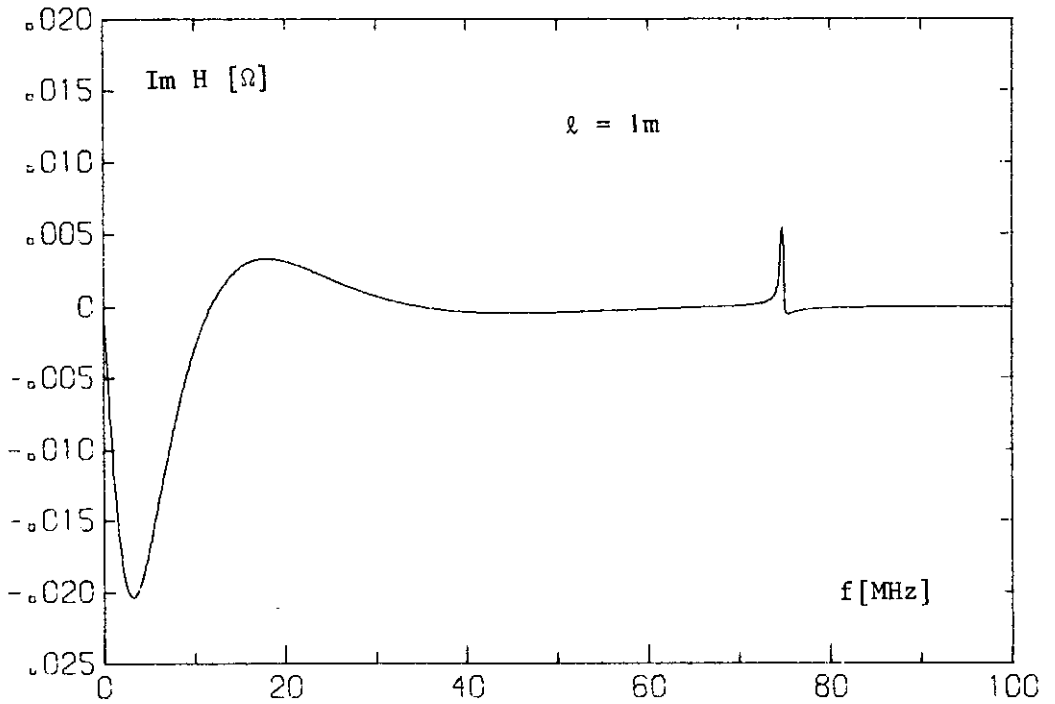


Fig.9b. The imaginary part of the transfer impedance as a function of frequency in 1000 steps of  $10^5$  Hz

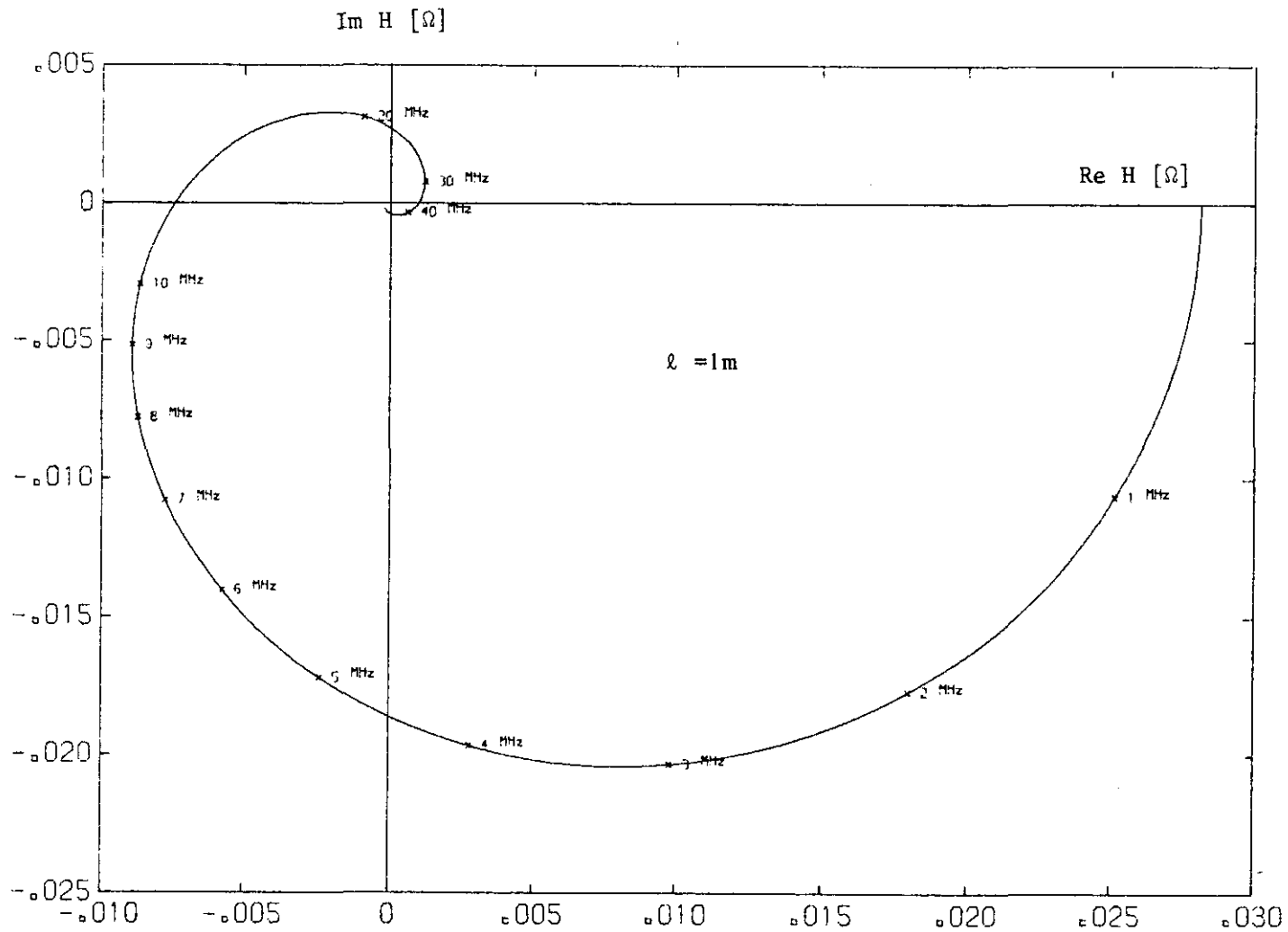


Fig.10. The polar plot of the transfer impedance in the complex plane with the frequency as a parameter

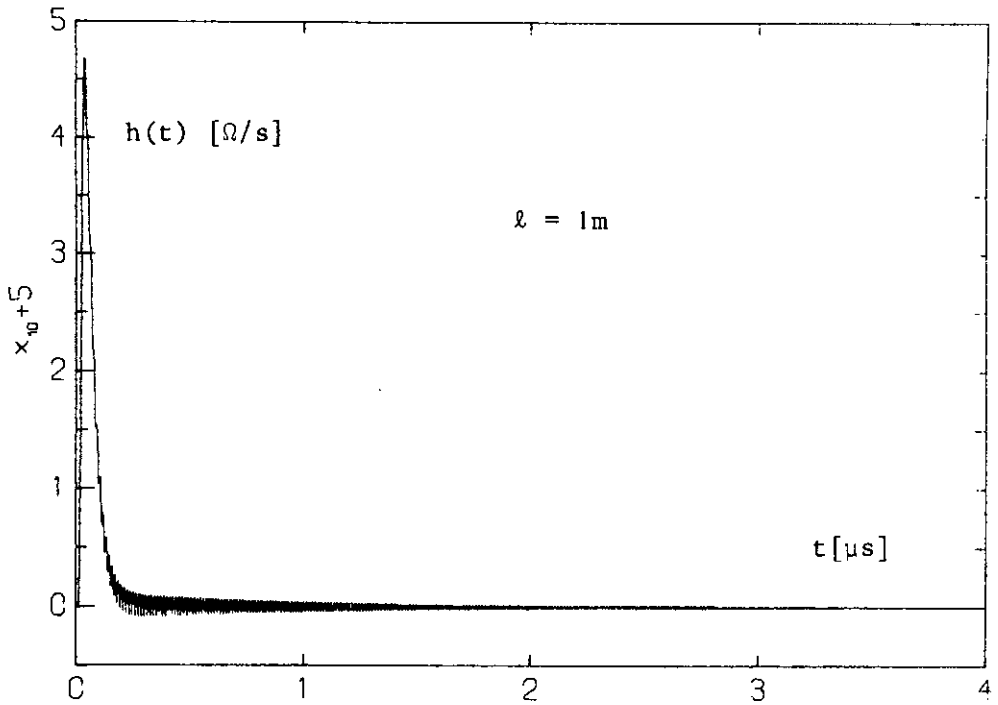


Fig.11a. The impulse response of the coaxial shunt; the result of an FFT of  $H(\omega)$ . The transform was performed with  $f_g = 500$  MHz and  $N=2048$ . Note that  $\Delta f$  is chosen small enough to ensure a negligible aliasing distortion.

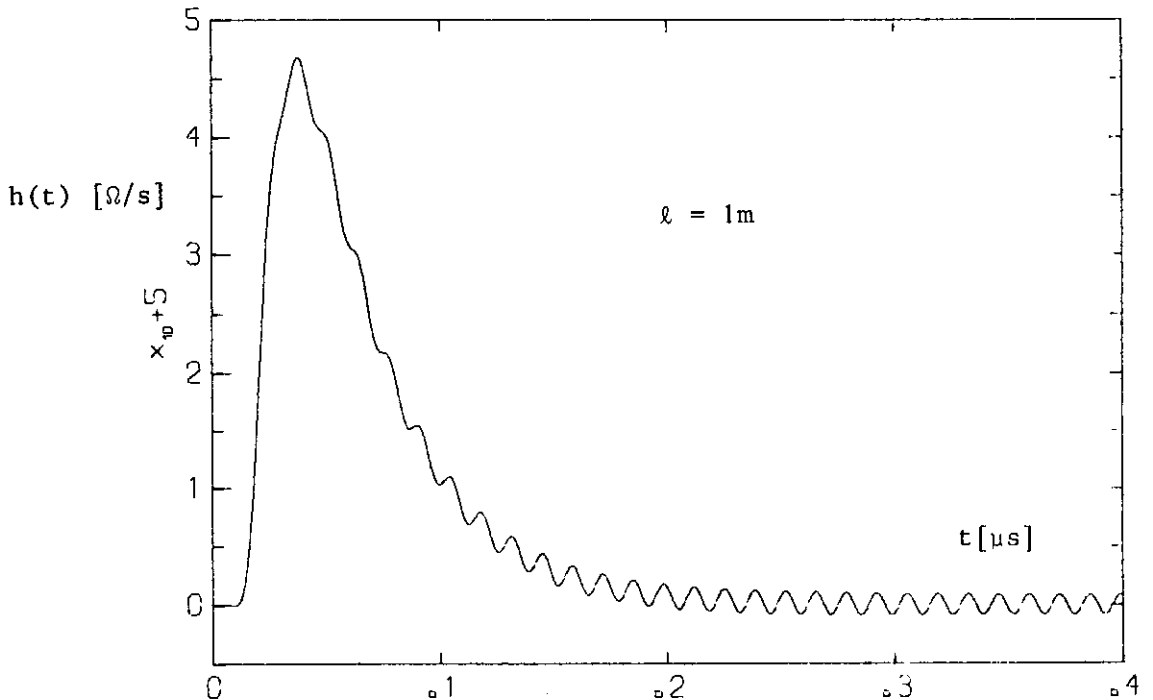


Fig.11b. The first part of the impulse response. Note the ripple of 75 MHz corresponding with the peak in the amplitude characteristic (fig.8a)

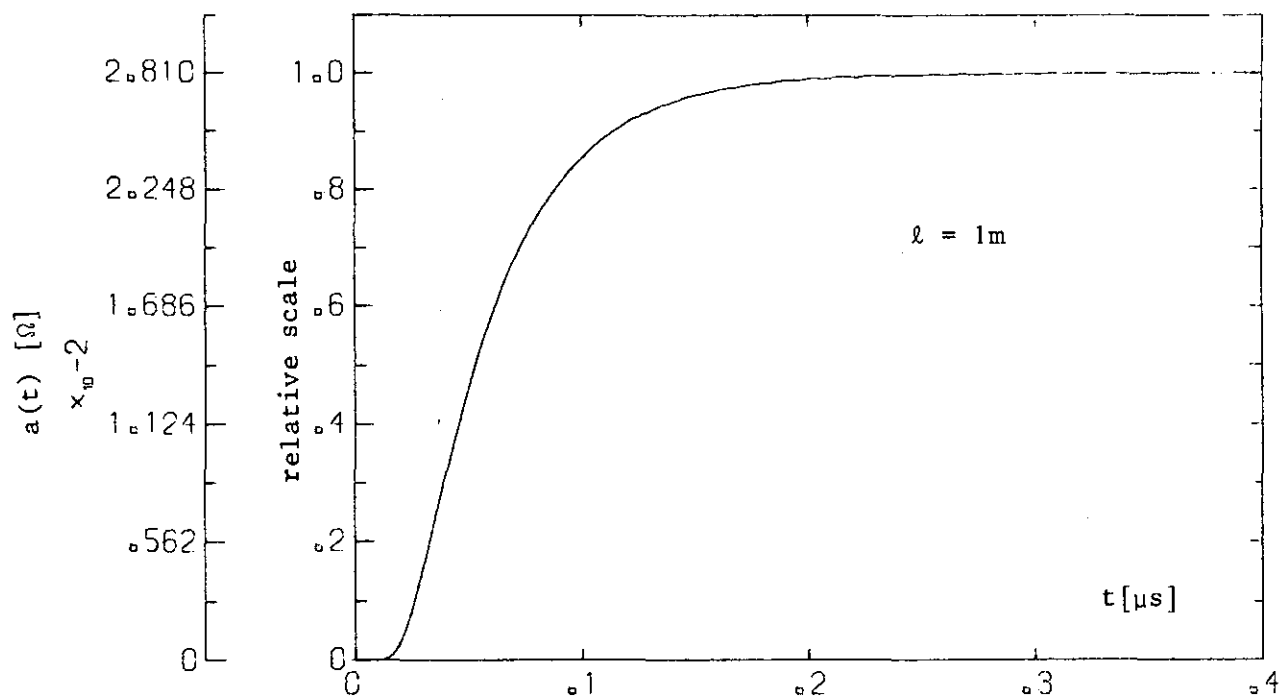


Fig.12. The step response of the coaxial shunt; the result of the integration of  $h(t)$

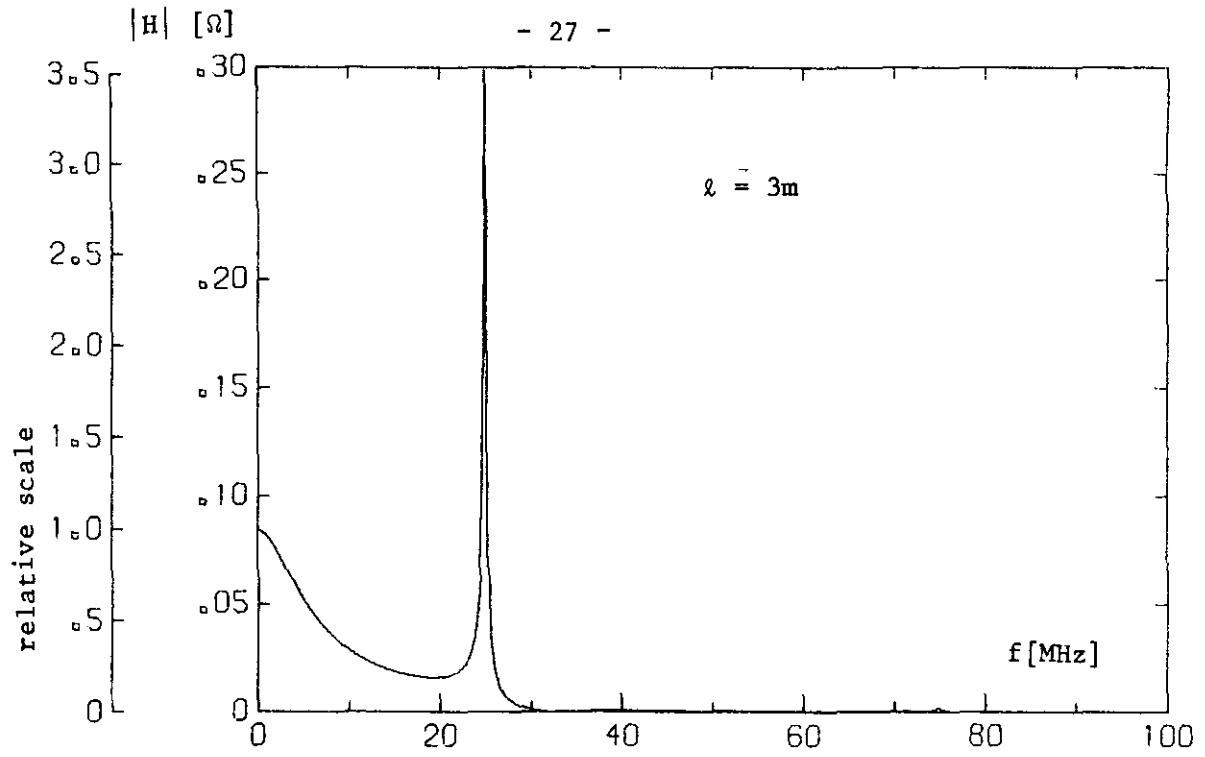


Fig. 13a. The amplitude characteristic of the transfer impedance, that is  $|H|=|V_a(l)/I|$  as a function of frequency in 1000 steps of  $10^5$  Hz. Note the peak at 25 MHz, corresponding with the shunt as a quarter wavelength line

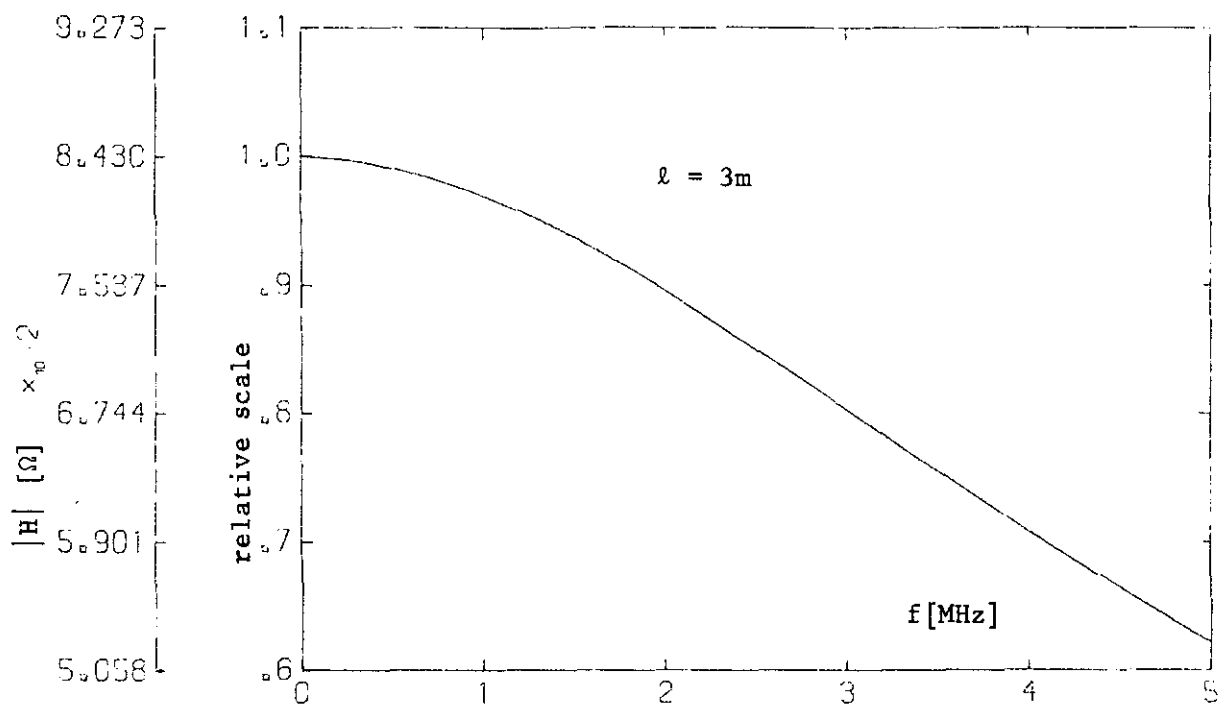


Fig. 13b. The low frequency part of the amplitude characteristic calculated in 100 steps of  $5 \cdot 10^4$  Hz

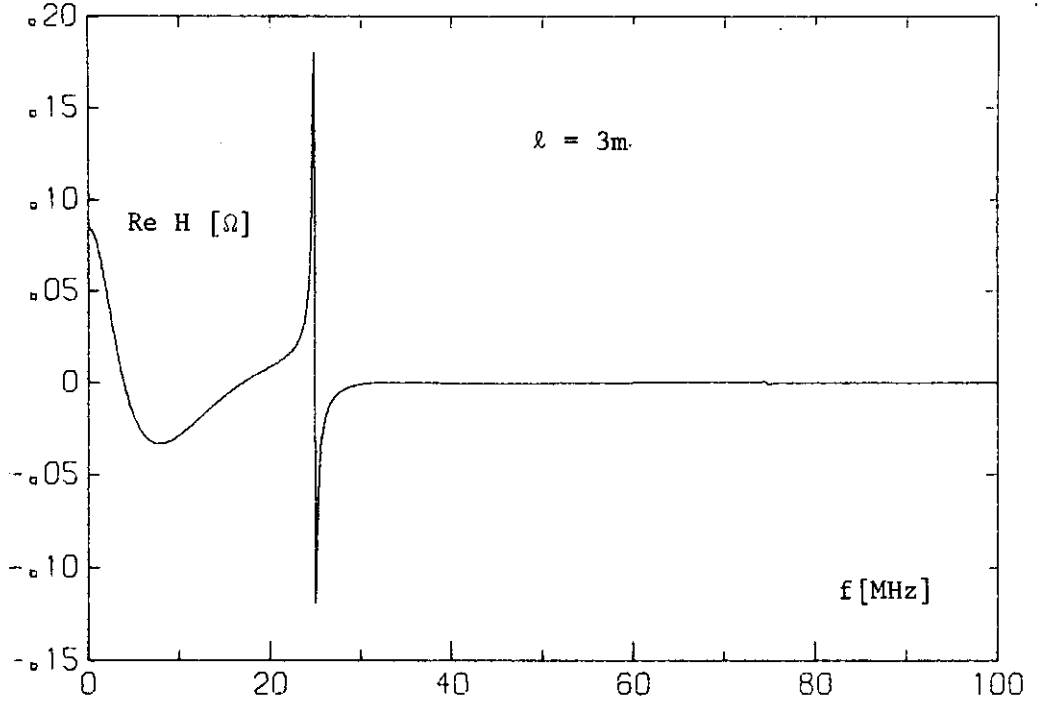


Fig. 14a. The real part of the transfer impedance as a function of frequency in 1000 steps of  $10^5$  Hz

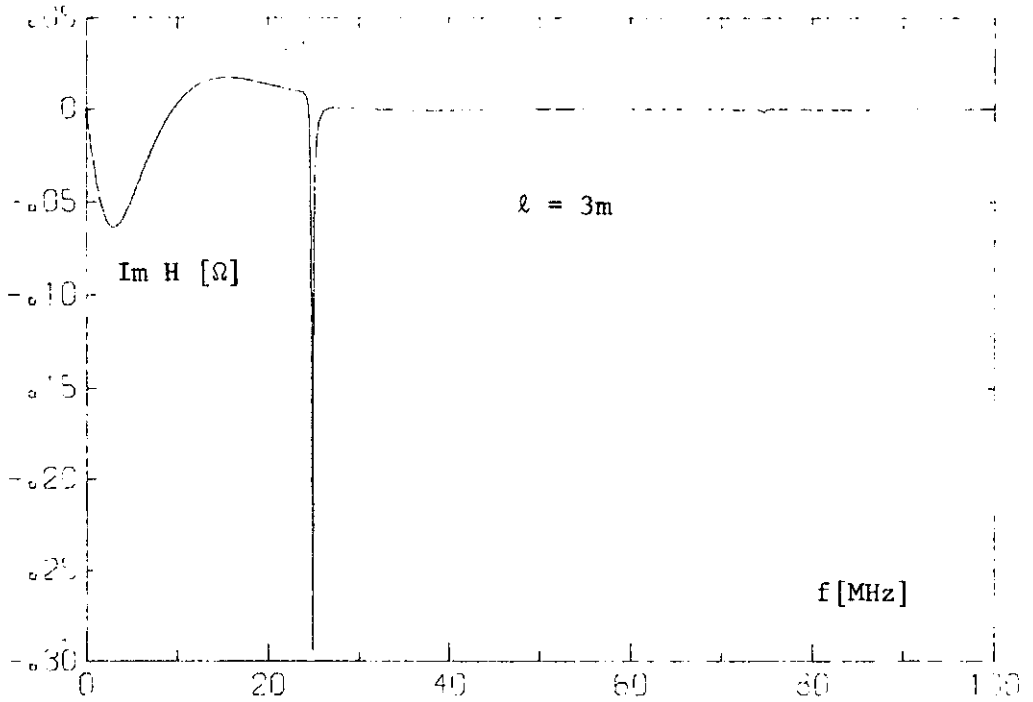


Fig. 14b. The imaginary part of the transfer impedance as a function of frequency in 1000 steps of  $10^5$  Hz



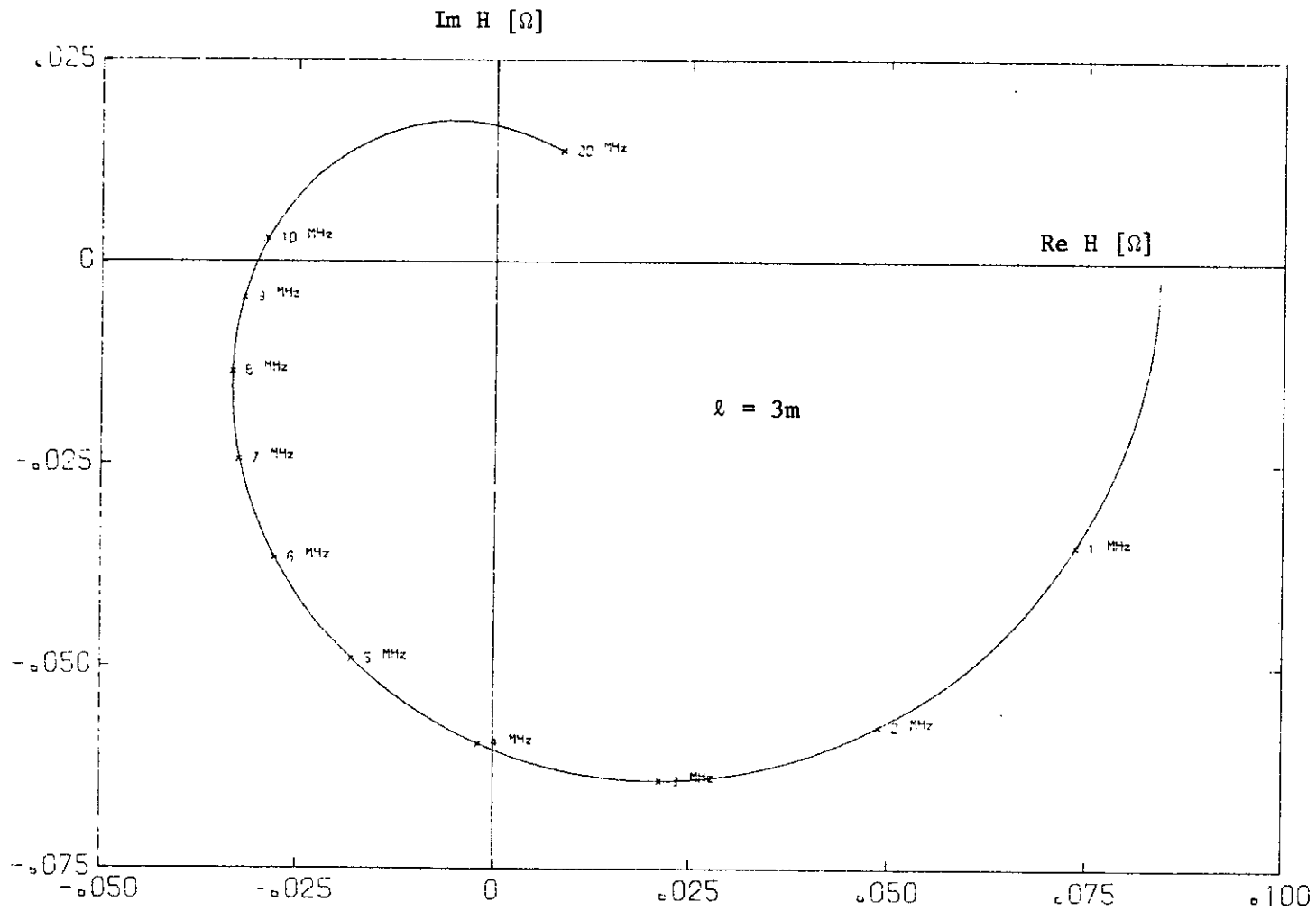


Fig. 15. The polar plot of the transfer impedance in the complex plane with the frequency as a parameter

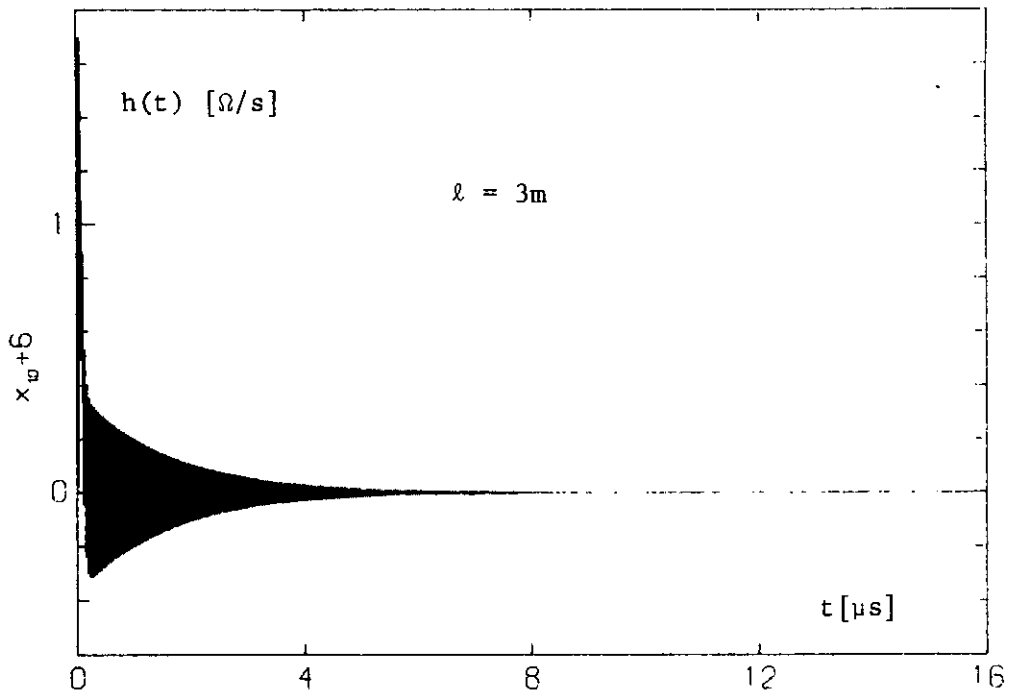


Fig. 16a. The impulse response of the coaxial shunt; the result of an FFT of  $H(\omega)$ . The transform was performed with  $f_g = 500$  MHz and  $N=8192$ . Note that  $\Delta f$  is chosen small enough to ensure a negligible aliasing distortion.

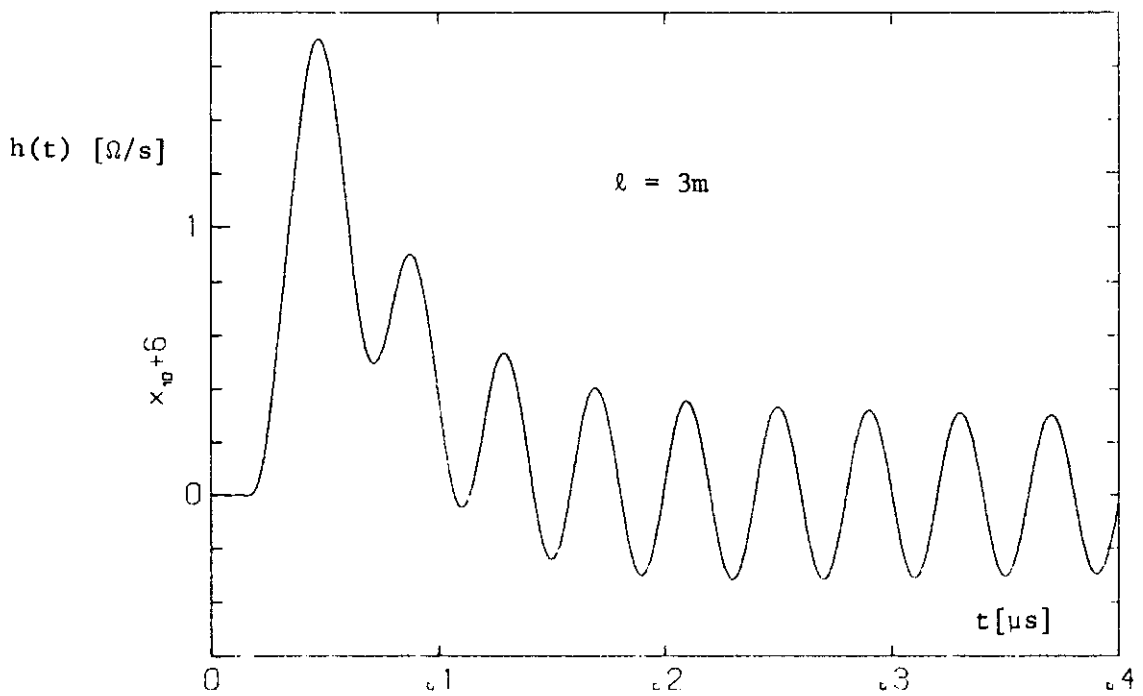


Fig. 16b. The first part of the impulse response. Note the ripple of 25 MHz corresponding with the peak in the amplitude characteristic (fig.13a)

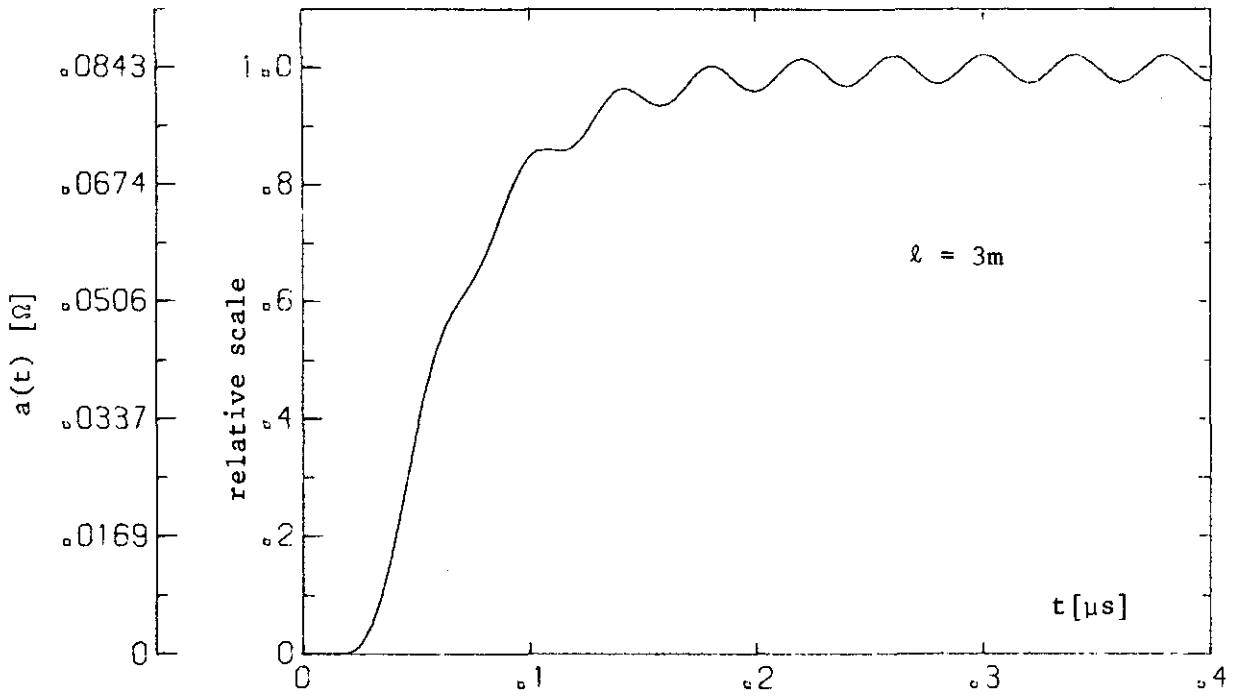


Fig. 17. The step response of the coaxial shunt; the result of the integration of  $h(t)$

## 9. Conclusions

1. The paper shows the possibility of a rigorous treatment of the coaxial shunt with the aid of the computer, without losing the possibility of physical interpretation.
2. The results of section 8 show clearly that the behaviour of the coaxial shunt in the high-frequency part of the frequency domain and related to this the first part of the impulse and step responses is influenced by the length of the coaxial shunt and is not exclusively a function of the wall thickness and the resistivity of the common conductor.
3. If the length of a coaxial shunt is of the order of the wavelength of the frequency concerned, it is not allowed to derive the transfer impedance of the two-port by simply multiplying the transfer impedance per unit length by the length of the shunt [3].  
(For the definition of the transfer impedance per unit length as a field intensity  $E$  divided by a current  $I$ , see Schelkunoff [2]).

10. Aknowledgement

The author appreciates the continued help and the interest of his colleague W.C. van Etten and is indebted to L. van der Waals whose competent and devoted efforts made it possible to conclude this work successfully.

11. References

1. John R. Carson and Ray S. Hoyt  
Propagation of periodic currents over a system of parallel wires.  
B.S.T.J. Vol. 6, no. 3, p. 495, July 1927.
2. S.A. Schelkunoff  
The electromagnetic theory of coaxial transmission lines and cylindrical shields.  
B.S.T.J. 13 July 1934.
3. John H. Park  
Shunts and inductors for surge-current measurements.  
Journal of research of the National Bureau of Standards - Research paper RP 1823. Volume 39, September 1947.
4. H. Kaden  
Wirbelströme und Schirmung in der Nachrichtentechnik.  
Springer-Verlag. Berlin 1959.
5. William T. Cochran et al.  
What is the fast Fourier transform ?  
Proc. of the I.E.E.E. vol. 55, no. 10, October 1967.
- 6 A. Schwab  
Hochspannungsmesstechnik, Berlin, Heidelberg, New York :  
Springer Verlag (1969).
7. B. Lago et al.  
Coaxial shunt  
Proc. of the I.E.E.E. vol. 114, No.9, September 1967

Reports:

- 1) Dijk, J., M. Jeuken and E.J. Maanders  
AN ANTENNA FOR A SATELLITE COMMUNICATION GROUND STATION  
(PROVISIONAL ELECTRICAL DESIGN). TH-report 68-E-01. March 1968.  
ISBN 90 6144 001 7
- 2) Veefkind, A., J.H. Blom and L.Th. Rietjens  
THEORETICAL AND EXPERIMENTAL INVESTIGATION OF A NON-EQUILIBRIUM  
PLASMA IN A MHD CHANNEL. TH-report 68-E-2. March 1968. Submitted  
to the Symposium on a Magnetohydrodynamic Electrical Power  
Generation, Warsaw, Poland, 24-30 July, 1968. ISBN 90 6144 002 5
- 3) Boom, A.J.W. van den and J.H.A.M. Melis  
A COMPARISON OF SOME PROCESS PARAMETER ESTIMATING SCHEMES.  
TH-report 68-E-03. September 1968. ISBN 90 6144 003 3
- 4) Eykhoff, P., P.J.M. Ophey, J. Severs and J.O.M. Oome  
AN ELECTROLYTIC TANK FOR INSTRUCTIONAL PURPOSES REPRESENTING THE  
COMPLEX-FREQUENCY PLANE. TH-report 68-E-04. September 1968.  
ISBN 90 6144 004 1
- 5) Vermij, L. and J.E. Daalder  
ENERGY BALANCE OF FUSING SILVER WIRES SURROUNDED BY AIR.  
TH-report 68-E-05. November 1968. ISBN 90 6144 005 X
- 6) Houben, J.W.M.A. and P. Masee  
MHD POWER CONVERSION EMPLOYING LIQUID METALS. TH-report 69-E-06.  
February 1969. ISBN 90 6144 006 8
- 7) Heuvel, W.M.C. van den and W.F.J. Kersten  
VOLTAGE MEASUREMENT IN CURRENT ZERO INVESTIGATIONS. TH-report 69-E-07.  
September 1969. ISBN 90 6144 007 6
- 8) Vermij, L.  
SELECTED BIBLIOGRAPHY OF FUSES. TH-report 69-E-08. September 1969.  
ISBN 90 6144 008 4
- 9) Westenberg, J.Z.  
SOME IDENTIFICATION SCHEMES FOR NON-LINEAR NOISY PROCESSES.  
TH-report 69-E-09. December 1969. ISBN 90 6144 009 2
- 10) Koop, H.E.M., J. Dijk and E.J. Maanders  
ON CONICAL HORN ANTENNAS. TH-report 70-E-10. February 1970.  
ISBN 90 6144 010 6
- 11) Veefkind, A.  
NON-EQUILIBRIUM PHENOMENA IN A DISC-SHAPED MAGNETOHYDRODYNAMIC  
GENERATOR. TH-report 70-E-11. March 1970. ISBN 90 6144 011 4
- 12) Jansen, J.K.M., M.E.J. Jeuken and C.W. Lambrechtse  
THE SCALAR FEED. TH-report 70-E-12. December 1969. ISBN 90 6144 012 2
- 13) Teuling, D.J.A.  
ELECTRONIC IMAGE MOTION COMPENSATION IN A PORTABLE TELEVISION CAMERA.  
TH-report 70-E-13. 1970. ISBN 90 6144 013 0

- 14) Lorencin, M.  
AUTOMATIC METEOR REFLECTIONS RECORDING EQUIPMENT. TH-report 70-E-14.  
November 1970. ISBN 90 6144 014 9
- 15) Smets, A.J.  
THE INSTRUMENTAL VARIABLE METHOD AND RELATED IDENTIFICATION SCHEMES.  
TH-report 70-E-15. November 1970. ISBN 90 6144 015 7
- 16) White, Jr., R.C.  
A SURVEY OF RANDOM METHODS FOR PARAMETER OPTIMIZATION. TH-report  
70-E-16. February 1971. ISBN 90 6144 016 5
- 17) Talmon, J.L.  
APPROXIMATED GAUSS-MARKOV ESTIMATIONS AND RELATED SCHEMES. TH-report  
71-E-17. February 1971. ISBN 90 6144 017 3
- 18) Kalásek, V.  
MEASUREMENT OF TIME CONSTANTS ON CASCADE D.C. ARC IN NITROGEN.  
TH-report 71-E-18. February 1971. ISBN 90 6144 018 1
- 19) Hosselet, L.M.L.F.  
OZONBILDUNG MITTELS ELEKTRISCHER ENTLADUNGEN. TH-report 71-E-19.  
March 1971. ISBN 90 6144 019 X
- 20) Arts, M.G.J.  
ON THE INSTANTANEOUS MEASUREMENT OF BLOODFLOW BY ULTRASONIC MEANS.  
TH-report 71-E-20. May 1971. ISBN 90 6144 020 3
- 21) Roer, Th.G. van de  
NON-ISO THERMAL ANALYSIS OF CARRIER WAVES IN A SEMICONDUCTOR.  
TH-report 71-E-21. August 1971. ISBN 90 6144 021 1
- 22) Jeuken, P.J., C. Huber and C.E. Mulders  
SENSING INERTIAL ROTATION WITH TUNING FORKS. TH-report 71-E-22.  
September 1971. ISBN 90 6144 022 X
- 23) Dijk, J. and E.J. Maanders  
APERTURE BLOCKING IN CASSEGRAIN ANTENNA SYSTEMS. A REVIEW.  
TH-report 71-E-23. September 1971. ISBN 90 6144 023 8
- 24) Kregting, J. and R.C. White, Jr.  
ADAPTIVE RANDOM SEARCH. TH-report 71-E-24. October 1971.  
ISBN 90 6144 024 6
- 25) Damen, A.A.H. and H.A.L. Piceni  
THE MULTIPLE DIPOLE MODEL OF THE VENTRICULAR DEPOLARISATION.  
TH-report 71-E-25. October 1971. ISBN 90 6144 025 4 (In preparation).
- 26) Bremmer, H.  
A MATHEMATICAL THEORY CONNECTING SCATTERING AND DIFFRACTION PHENOMENA,  
INCLUDING BRAGG-TYPE INTERFERENCES. TH-report 71-E-26. December 1971.  
ISBN 90 6144 026 2
- 27) Bokhoven, W.M.G. van  
METHODS AND ASPECTS OF ACTIVE-RC FILTERS SYNTHESIS. TH-report 71-E-27.  
10 December 1970. ISBN 90 6144 027 0
- 28) Boeschoten, F.  
TWO FLUIDS MODEL REEXAMINED. TH-report 72-E-28. March 1972.  
ISBN 90 6144 028 9



- 29) REPORT ON THE CLOSED CYCLE MHD SPECIALIST MEETING. Working group of the joint ENEA/IAEA international MHD liaison group. Eindhoven, The Netherlands, September 20-22, 1971. Edited by L.H.Th. Rietjens. TH-report 72-E-29. April 1972. ISBN 90 6144 029 7
- 30) Kessel, C.G.M. van and J.W.M.A. Houben  
LOSS MECHANISMS IN AN MHD GENERATOR. TH-report 72-E-30. June 1972. ISBN 90 6144 030 0
- 31) Veefkind, A.  
CONDUCTING GRIDS TO STABILIZE MHD GENERATOR PLASMAS AGAINST IONIZATION INSTABILITIES. TH-report 72-E-31. September 1972. ISBN 90 6144 031 9
- 32) Daalder, J.E. and C.W.M. Vos  
DISTRIBUTION FUNCTIONS OF THE SPOT DIAMETER FOR SINGLE- AND MULTI-CATHODE DISCHARGES IN VACUUM. TH-report 73-E-32. January 1973. ISBN 90 6144 032 7
- 33) Daalder, J.E.  
JOULE HEATING AND DIAMETER OF THE CATHODE SPOT IN A VACUUM ARC. TH-report 73-E-33. January 1973. ISBN 90 6144 033 5
- 34) Huber, C.  
BEHAVIOUR OF THE SPINNING GYRO ROTOR. TH-report 73-E-34. February 1973. ISBN 90 6144 034 3
- 35) Bastian, C. et al.  
THE VACUUM ARC AS A FACILITY FOR RELEVANT EXPERIMENTS IN FUSION RESEARCH. Annual Report 1972. EURATOM-T.H.E. Group "Rotating Plasma". TH-report 73-E-35. February 1973. ISBN 90 6144 035 1
- 36) Blom, J.A.  
ANALYSIS OF PHYSIOLOGICAL SYSTEMS BY PARAMETER ESTIMATION TECHNIQUES. 73-E-36. May 1973. ISBN 90 6144 036 X
- 37) Lier, M.C. van and R.H.J.M. Otten  
AUTOMATIC WIRING DESIGN. TH-report 73-E-37. May 1973. ISBN 90 6144 037 8 (vervalt zie 74-E-44)
- 38) Andriessen, F.J., W. Boerman and I.F.E.M. Holtz  
CALCULATION OF RADIATION LOSSES IN CYLINDRICAL SYMMETRICAL HIGH PRESSURE DISCHARGES BY MEANS OF A DIGITAL COMPUTER. TH-report 73-E-38. October 1973. ISBN 90 6144 038 6
- 39) Dijk, J., C.T.W. van Diepenbeek, E.J. Maanders and L.F.G. Thurlings  
THE POLARIZATION LOSSES OF OFFSET ANTENNAS. TH-report 73-E-39. June 1973. ISBN 90 6144 039 4 (in preparation)
- 40) Goes, W.P.  
SEPARATION OF SIGNALS DUE TO ARTERIAL AND VENOUS BLOOD FLOW IN THE DOPPLER SYSTEM THAT USES CONTINUOUS ULTRASOUND. TH-report 73-E-40. September 1973. ISBN 90 6144 040 8
- 41) Damen, A.A.H.  
COMPARATIVE ANALYSIS OF SEVERAL MODELS OF THE VENTRICULAR DE-POLARISATION; INTRODUCTION OF A STRING-MODEL. TH-report 73-E-41. October 1973. ISBN 90 6144 041 6

- 42) Dijk, G.H.M. van  
THEORY OF GYRO WITH ROTATING GIMBAL AND FLEXTURAL PRIOTS.  
TH-report 73-E-42. November 1973. ISBN 90 6144 042 4
- 43) Breimer, A.J.  
ON THE IDENTIFICATION OF CONTINUOUS LINEAR PROCESSES. TH-report  
74-E-43, January 1974. ISBN 90 6144 043 2
- 44) Lier, M.C. van and R.H.J.M. Otten  
CAD OF MASKS AND WIRING. TH-report 74-E-44. February 1974.  
ISBN 90 6144 044 0
- 45) Bastian, C. et al.  
EXPERIMENTS WITH A LARGE SIZED HOLLOW CATHODE DISCHARGE FED WITH  
ARGON. Annual Report 1973. EURATOM-T.H.E. Group "Rotating Plasma".  
TH-report 74-E-45. April 1974. ISBN 90 6144 045 9
- 46) Roer, Th.G. van de  
ANALYTICAL SMALL-SIGNAL THEORY OF BARITT DIODES. TH-report 74-E-46.  
May 1974. ISBN 90 6144 046 7
- 47) Leliveld, W.H.  
THE DESIGN OF A MOCK CIRCULATION SYSTEM. TH-report 74-E-47. June 1974.  
ISBN 90 6144 047 5
- 48) Damen, A.A.H.  
SOME NOTES ON THE INVERSE PROBLEM IN ELECTRO CARDIOGRAPHY. TH-report  
74-E-48. July 1974. ISBN 90 6144 048 3
- 49) Meeberg, L. van de  
A VITERBI DECODER. TH-report 74-E-49. October 1974. ISEN 90 6144 049 1
- 50) Poel, A.P.M. van der  
A COMPUTER SEARCH FOR GOOD CONVOLUTIONAL CODES. TH-report 74-E-50.  
October 1974. ISBN 90 6144 050 3
- 51) Sampic, G.  
THE BIT ERROR PROBABILITY AS A FUNCTION PATH REGISTER LENGTH IN THE  
VITERBI DECODER. TH-report 74-E-51. October 1974. ISBN 90 6144 051 3
- 52) Schalkwijk, J.P.M.  
CODING FOR A COMPUTER NETWORK. TH-report 74-E-52. October 1974.  
ISBN 90 6144 052 1
- 53) Stapper, M.  
MEASUREMENT OF THE INTENSITY OF PROGRESSIVE ULTRASONIC WAVES BY MEANS  
OF RAMAN-NATH DIFRACTION. TH-report 74-E-53. November 1974.  
ISBN 90 6144 053 X
- 54) Schalkwijk, J.P.M. and A.J. Vinck  
SYNDROME DECODING OF CONVOLUTIONAL CODES. TH-report 74-E-54.  
November 1974. ISBN 90 6144 054 8
- 55) Yakimov, A.  
FLUCTUATIONS IN IMPATT-DIODE OSCILLATORS WITH LOW  $q$ -SECTORS.  
TH-report 7--E-55. November 1974. ISBN 90 6144 054 6